

Single-file diffusion in a bi-stable potential: signatures of memory in the barrier-crossing of a tagged-particle

Alessio Lapolla¹ and Aljaž Godec^{1, a)}

Mathematical bioPhysics Group, Max Planck Institute for Biophysical Chemistry, Am Fassberg 11, 37077 Göttingen, Germany

We investigate memory effects in barrier-crossing in the overdamped setting. We focus on the scenario where the hidden degrees of freedom relax on exactly the same time scale as the observable. As a prototypical model we analyze tagged-particle diffusion in a single-file confined to a bi-stable potential. We identify the signatures of memory and explain their origin. The emerging memory is a result of the projection of collective many-body eigenmodes onto the motion of a tagged-particle. We are interested in the 'confining' (all background particles in front of the tagged-particle) and 'pushing' (all background particles behind the tagged-particle) scenarios for which we find non-trivial and qualitatively different relaxation behavior. Notably and somewhat unexpectedly, at fixed particle number we find that the higher the barrier the more prominent are the signatures of memory. Our results can readily be tested experimentally and may be relevant for understanding transport in biological ion-channels.

I. INTRODUCTION

Non-linear stochastic flows are at the heart of thermally driven processes in systems whose potential energy surfaces are characterized by multiple local energy minima. Pioneered by the seminal work of Kramers¹ the concept of thermally activated barrier-crossing has ever since been applied to diverse phenomena, incl. chemical reactions²⁻⁴, tunnel-diodes⁵, laser-pumping⁶, magnetic resonance⁷, conformational dynamics and folding of proteins⁸⁻¹⁶ and nucleic acids^{17,18} and receptor-ligand binding¹⁹, to name but a few.

From a theoretical point of view, the most detailed and precise results were obtained in the context of relaxation phenomena²⁰⁻²⁶ and first passage time statistics²⁷⁻³⁴ in Markovian (i.e. memory-less) systems. However, physical observables typically correspond to lower-dimensional projections and the observed dynamics is Markovian only under quite restrictive conditions on the nature of the projection³⁵. Quoting van Kampen: "Non-Markov is the rule, Markov is the exception"³⁶.

Over the years non-Markovian barrier crossing has therefore received special attention. Most approaches considered a generalized Langevin equation in the underdamped regime with diverse phenomenological memory kernels for the velocity in the high³⁷⁻³⁹ and low^{40,41} viscosity limit. In the case of diffusion in double-well potentials unified solutions have been obtained⁴². Seminal results on non-Markovian effects in the crossing of high energy barriers have been obtained by Mel'nikov and Meshkov⁴³, and were later extended to low barriers by Kalmykov, Coffey and Titov⁴⁴. Important results on non-Markovian barrier-crossing have been obtained in the context of condensed-phase dynamics^{45,46}. More recent studies of memory effects in bi-stable potentials have been carried out in the context of conformational dynamics of macromolecules^{16,47} and the role of hydrodynamic memory in surmounting energy barriers⁴⁸, while recent applications involve the interpretation of experiments on the folding of a DNA hairpin⁴⁹.

Quite detailed analytical results have also been obtained for overdamped non-Markovian stochastic flows in bi-stable potentials, in particular for exponentially correlated noise⁵⁰⁻⁵⁴. Characteristic of these studies is that the memory is introduced phenomenologically and/or the systems typically possess slow and fast degrees of freedom. Thereby, integrating out of fast degrees of freedom leads to memory, and time-scales similar to, or longer than, the correlation time are of interest.

Here, we are interested in the scenario where the background degrees of freedom (i.e. those that become integrated out) relax on exactly the same time scale as the observable. In particular, we are interested in the relaxation dynamics of a tagged-particle in a single-file of Brownian particles confined to a bi-stable potential, and investigate the rôle of the height of the potential barrier. Projecting out particles' positions introduces memory and strongly breaks Markovianity³⁵. The more particles' coordinates become integrated out the stronger Markovianity is broken³⁵. A distinguishing characteristic of our approach with respect to the existing literature is, therefore, that we do not introduce memory phenomenologically via a generalized Langevin equation. Instead, the memory arises explicitly as a result of projecting out degrees of freedom in an exactly solvable Markovian many-body system.

Single-file models are generically used to describe strongly correlated, effectively one-dimensional, systems and processes, e.g. biological channels⁵⁵, transport in zeolites⁵⁶, crowding effects in gene regulation^{57,58}, superionic conductors⁵⁹, and strongly correlated one-dimensional soft matter systems in general⁶⁰. Over the past years diverse theoretical studies yielded deep insight about the anomalous tagged-particle diffusion⁶¹⁻⁶⁹ and the emergence and meaning of memory^{35,70,71}. Single-file diffusion in potential landscapes has been studied by computer simulations⁷². However, the rôle of crowding/steric obstruction and particle correlations in barrier-crossing, and in particular in the relaxation towards equilibrium, has so far remained elusive.

In this work we provide in Sec. II an analytical solution to the problem using the coordinate Bethe ansatz. In Sec. III we analyze the equilibrium correlation time as a function of the barrier height and number of particles in the single-file. Sec. IV addresses the relaxation to equilibrium from a fixed,

^{a)}agodec@mpibpc.mpg.de

non-equilibrium initial condition of the tagged-particle in the 'confining' and 'pushing' scenario, respectively. We conclude with a brief discussion incl. potential applications and extensions of our results.

II. THEORY

We consider a single-file of N point-particles confined to a box of length $L = 2\pi$. In the center of the box there is a square-top energy barrier of width π and height U_b (see Fig. 1a). More precisely, each particle experiences the potential^{73,74}

$$U(x) = \begin{cases} 0, & \pi > |x| > \pi/2 \\ U_b, & |x| \leq \pi/2 \\ \infty, & \text{otherwise.} \end{cases} \quad (1)$$

The particles move according to overdamped Brownian dynamics under non-crossing conditions. For simplicity and without loss of generality we set $D = 1$, which is equivalent to expressing time in units of $4\pi^2/D$, and express U in units of thermal energy $k_B T$, i.e. $U \rightarrow U/k_B T$. The probability density of the set of positions $\{x_i\} = \mathbf{x}$ of the N particles evolves according to the many-body Fokker-Planck equation

$$\left(\partial_t - \sum_{i=1}^N [\partial_{x_i}^2 + \partial_{x_i} \{ \partial_{x_i} U(x_i) \}] \right) G(\mathbf{x}, t | \mathbf{x}_0) = 0, \quad (2)$$

with initial condition $G(\mathbf{x}, 0 | \mathbf{x}_0) = \prod_{i=1}^N \delta(x_i - x_{0i})$ and where the operator in curly brackets $\{\}$ acts only within the bracket. Eq. (2) is equipped with the set of external and internal boundary conditions

$$\begin{aligned} \partial_{x_1} G(\mathbf{x}, t | \mathbf{x}_0)|_{x_1=-\pi} &= \partial_{x_N} G(\mathbf{x}, t | \mathbf{x}_0)|_{x_N=\pi} = 0 \\ (\partial_{x_{i+1}} - \partial_{x_i}) G(\mathbf{x}, t | \mathbf{x}_0)|_{x_{i+1}=x_i} &= 0, \end{aligned} \quad (3)$$

and is solved exactly using the coordinate Bethe ansatz (for technical details refer to Refs. 35, 71, and 75). The resulting many-body Green's function reads

$$G(\mathbf{x}, t | \mathbf{x}_0) = \sum_{\mathbf{k}} \Psi_{\mathbf{k}}^R(\mathbf{x}) \Psi_{\mathbf{k}}^L(\mathbf{x}_0) e^{-\Lambda_{\mathbf{k}} t} \quad (4)$$

where $\Psi_{\mathbf{k}}^L(\mathbf{x})$ and $\Psi_{\mathbf{k}}^R(\mathbf{x})$ are the so-called left and right Bethe eigenfunctions, respectively, defined as

$$\Psi_{\mathbf{k}}^{L,R}(\mathbf{x}) \equiv \mathcal{N}^{1/2} \hat{O}_{\mathbf{x}} \sum_{\{\mathbf{k}\}} \prod_{i=1}^N \psi_{k_i}^{L,R}(x_i), \quad (5)$$

where $\psi_n^{L,R}(x)$ are the orthonormal eigenfunctions of the single-particle problem (given in Appendix), the sum over $\{\mathbf{k}\}$ refers to the sum over all permutations of the multiset \mathbf{k} , and \mathcal{N} is the number of these permutations \mathbf{k} . $\Lambda_{\mathbf{k}} = \sum_{i=1}^N \lambda_{k_i}$ refers to the Bethe eigenvalue with multi-index $\mathbf{k} = \{k_i\}$, $i \in [1, N]$, and $\hat{O}_{\mathbf{x}}$ is the particle-ordering operator, which ensures

that $x_1 \leq \dots \leq x_i \leq \dots \leq x_N$. Moreover, λ_n refer to the eigenvalues of the respective one-body problem given by^{73,74}

$$\lambda_n = \begin{cases} \frac{n^2}{4}, & \text{mod}(n, 4) = 0, \\ \left(\frac{n-1}{2} + v \right)^2, & \text{mod}(n, 4) = 1, \\ \frac{n^2}{4}, & \text{mod}(n, 4) = 2, \\ \left(\frac{n+1}{2} - v \right)^2, & \text{mod}(n, 4) = 3 \end{cases} \quad (6)$$

where $v = 2 \arctan(e^{-U_b/2})/\pi$ and $\text{mod}(k, l)$ stands for the remainder of the division k/l .

We are interested in the non-Markovian probability density of x_i , the position of the i -th tagged-particle under the condition that the initial positions of the remaining particles are drawn from those equilibrium configurations that contain particle i at x_0 , which reads (for a derivation see 35, 71, and 75)

$$\mathcal{G}(x_i, t | x_{0i}) = V_{\mathbf{00}}^{-1}(x_{0i}) \sum_{\mathbf{k}} V_{\mathbf{0k}}(x_i) V_{\mathbf{k0}}(x_{0i}) e^{-\Lambda_{\mathbf{k}} t}, \quad (7)$$

where the 'overlap-elements' $V_{\mathbf{kl}}(x_i)$ are defined as⁷⁵

$$V_{\mathbf{kl}}(x_i) = \frac{m_{\mathbf{l}}}{N_L! N_R!} \sum_{\{\mathbf{k}\}} \sum_{\{\mathbf{l}\}} \Psi_{k_i}^R(x_i) \Psi_{l_i}^L(x_i) \prod_{n=1}^{i-1} L_n(x_i) \prod_{m=i+1}^N R_m(x_i) \quad (8)$$

with $m_{\mathbf{l}}$ being the multiplicity of the multiset \mathbf{l} , and $N_L = i - 1$ and $N_R = N - i$ are, respectively, the number of particles to the left and right of the tagged-particle. In Eq. (8) we introduced the auxiliary functions

$$L_n(x) = \int_{-\pi}^x dz \psi_n^L(z) \psi_{k_n}^R(z), \quad R_n(x) = \int_x^{\pi} dz \psi_n^L(z) \psi_{k_n}^R(z). \quad (9)$$

Note that the equilibrium probability density of the tagged-particle's position is given by (see Eq. (7)) $\mathcal{P}_{\text{eq}}(x_i) \equiv \lim_{t \rightarrow \infty} \mathcal{G}(x_i, t | x_{0i}) = V_{\mathbf{00}}(x_i)$ and is depicted for various values of U_b in Fig. 1b-d. Intuitively, as U_b increases particles become expelled from the barrier.

In Ref. 75 we have developed an algorithm designed to efficiently cope with the combinatorial complexity of the implementation of the analytical solution in Eq. (7). Due to the piece-wise constant nature of the potential $U(x)$ in Eq. (1) all integrals (9) can be computed analytically. As the resulting expressions are lengthy we do not show them here. Instead, they are readily implemented in an extension of the code published in Ref. 75 (see Supplementary Material).

III. LINEAR CORRELATIONS AT EQUILIBRIUM

First we consider linear correlations at equilibrium and limit the discussion in the reminder of the paper to tagging the first or last particle (i.e. throughout we set $i = 1$ or $i = N$).

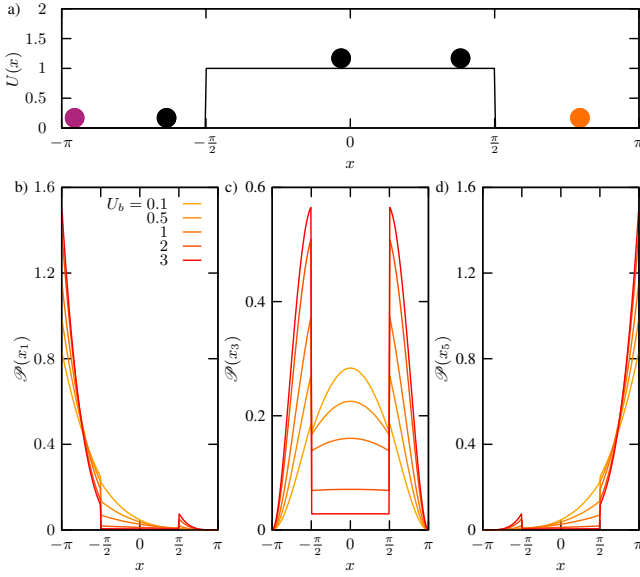


FIG. 1. a) Schematic of the potential $U(x)$ defined in Eq. (1); Single-file with $N = 5$ particles. Throughout this work we either tag the first (magenta stands for $i = 1$) or the last (orange stands for $i = N$) particle. b), c) and d) depict, respectively, the equilibrium probability distribution $\mathcal{P}_{\text{eq}}(x_i)$ for $i = 1$ (b) $i = 3$ (c) and $i = 5$ (d) in a single-file with $N = 5$ for different barrier heights U_b .

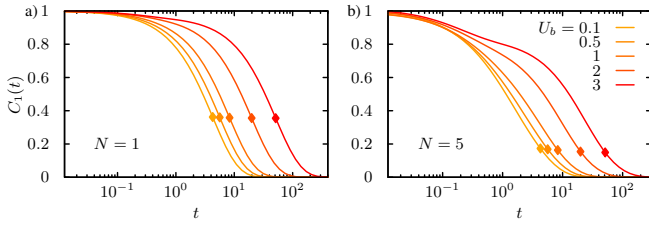


FIG. 2. Position autocorrelation function $C_1(t)$ of an isolated particle (a) and the leftmost tagged-particle in a single-file with five particles (b) as a function of the barrier height U_b . Symbols denote $C_1(\Lambda_1^{-1})$.

That is, we are interested in the normalized positional autocorrelation function of a tagged-particle defined as

$$C_i(t) = \frac{\langle x_i(t)x_i(0) \rangle - \langle x_i \rangle^2}{\langle x_i^2 \rangle - \langle x_i \rangle^2}, \quad (10)$$

where the covariance of the position is defined as

$$\langle x_i(t)x_i(0) \rangle \equiv \int_{-\pi}^{\pi} dx_i \int_{-\pi}^{\pi} dx_{0i} x_i x_{0i} \mathcal{G}(x_i, t | x_{0i}) \mathcal{P}_{\text{eq}}(x_{0i}), \quad (11)$$

and $\langle x_i^n \rangle = \int_{-\pi}^{\pi} dx_i x_i^n \mathcal{P}_{\text{eq}}(x_i)$. The above integrals have been performed numerically by means of Gauss-Kronrod quadrature⁷⁶. Note that Eq. (10) alongside Eqs. (5-9) necessarily implies the structure $C_i(t) = \sum_{\mathbf{k}} a_{\mathbf{k}} e^{-\Lambda_{\mathbf{k}} t}$ with $\sum_{\mathbf{k}} a_{\mathbf{k}} = 1$ and where all $a_{\mathbf{k}} \geq 0$ ⁷⁷. The results for $C_1(t)$ as a function of the barrier height U_b are depicted in Fig. 2. Since $U(x)$ is symmetric the autocorrelation functions of the first and last particle coincide, i.e. $C_1(t) = C_N(t)$.

The autocorrelation of an isolated particle (i.e. $N = 1$) in Fig. 2a displays for a given value of U_b to a good approximation an exponential decay with rate $\Lambda_1 = \lambda_1$ given by Eq. (6). This reflects that positional correlations decay predominantly due to barrier-crossing. Conversely, as the number of particles increases $C_1(t)$ decays on multiple time-scales (see Fig. 2b) and develops an ‘‘anomalous’’ shoulder on shorter time-scales⁷⁰, whose span increases with the barrier height U_b . A comparison of $C_1(\Lambda_1^{-1})$ reveals that the relative decay of correlations from the relaxation time $\tau_{\text{rel}} \equiv \Lambda_1^{-1}$ onward is substantially reduced for about a factor of 2 compared to the isolated particle case. τ_{rel} denotes the time-scale on which the system reaches equilibrium from any initial condition. Note that (i) $C_1(t)$ measures relative correlations and (ii) according to Eq. (7) (terminal) relaxation roughly corresponds to the particles individually crossing the barrier several times. It is also important to note that the natural time-scale of a tagged-particle is set by the average collision time^{35,71} $\tau_{\text{col}} = 1/N^2$ which decreases with increasing N . That is, in units of the average number of collisions $t \rightarrow t/\tau_{\text{col}}$ correlations decay more slowly for larger N .

A common means to quantify the extent of correlations found in the literature is the so-called *correlation time* T_c ^{25,26,44,78} and should be compared with the actual relaxation time τ_{rel} ⁷⁹

$$T_c = \int_0^{\infty} dt C_i(t), \quad \tau_{\text{rel}} \equiv \Lambda_1^{-1} = \left(\frac{2}{\pi} \arctan(e^{-U_b/2}) \right)^{-2}, \quad (12)$$

where we note that for high barriers, i.e. $U_b \gg 1$, the relaxation time follows the expected Arrhenius scaling $\tau_{\text{rel}} \simeq 4e^{U_b}/\pi^2$. In Fig. 3a we depict the correlation time for the leftmost particle in units of τ_{col} as a function of the barrier height U_b for different N . For an isolated particle $T_c = T_c^{\text{isolated}}$ agrees very well with τ_{rel} for all values of U_b , confirming the idea that $C(t)$ decays to a very good approximation as a single exponential. Note that, for systems obeying detailed balance, the mathematical structure of $C_i(t)$ trivially implies a shorter correlation time as soon as $C_i(t)$ decays on multiple time-scales if the longest time-scale Λ_1^{-1} is the same. This is particularly true when comparing $C_i(t)$ of a tagged-particle in a single-file with an isolated particle. Namely,

$$T_c = \sum_{\mathbf{k}} a_{\mathbf{k}} / \Lambda_{\mathbf{k}} \leq \sum_{\mathbf{k}} a_{\mathbf{k}} / \Lambda_1 = \Lambda_1^{-1} \approx T_c^{\text{isolated}}. \quad (13)$$

Therefore, the interpretation of T_c should always be made cautiously and in the particular case of tagged-particle diffusion in a single-file is not meaningful if we consider T_c on an absolute scale. However, it becomes somewhat more meaningful on the natural time-scale, i.e. when time is expressed in terms of the average number of inter-particle collisions (see also 35). Inspecting $C_1(t)$ on this natural time scale we find in Fig. 3a that the tagged-particle on average undergoes more collisions before it decorrelates for larger values of N , and this number increases with increasing U_b .

Moreover, as N increases the space explored by a tagged-particle becomes progressively more confined³⁵ rendering the correlation time T_c on an absolute time-scale also intuitively

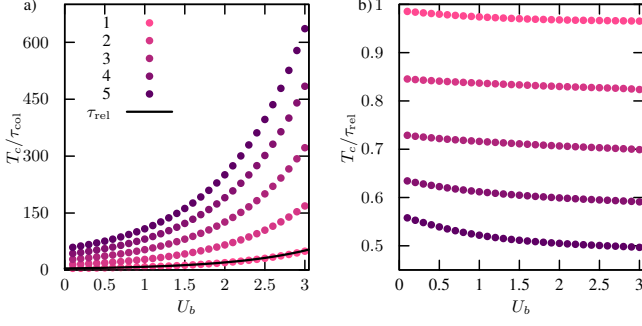


FIG. 3. a) T_c/τ_{col} for the first particle (i.e. $i = 1$) as a function of the barrier-height U_b for various values of N ; The full line depicts $\tau_{\text{rel}} \equiv \Lambda_1^{-1}$. b) Ratio T_c/τ_{rel} as a function of the barrier-height U_b for various values of N .

shorter. Indeed, in Fig. 3b we depict the ratio T_c/Λ_1^{-1} which decreases with increasing N for any barrier height U_b . Note that Λ_1^{-1} is independent of N and the breaking of Markovianity (reflected, e.g. in the violation of the Chapman-Kolmogorov semi-group property³⁵) is encoded entirely in the overlap elements $V_{0\mathbf{k}}, V_{\mathbf{k}0}$. For systems with microscopically reversible dynamics $T_c/\Lambda_1^{-1} < 1$ quite generally implies that relaxation evolves on multiple time-scales. Thus, the results in Fig. 3b suggest, in agreement with intuition, that more and more time-scales are involved in the relaxation of a tagged-particle's position in equilibrium as we increase N . In other words, on the level of linear correlations signatures of memory of the initial conditions of 'latent'/background particles are reflected in the multi-scale relaxation of $C_1(t)$.

IV. RELAXATION FROM A PINNED CONFIGURATION

We now focus on the 'complete' (i.e. incl. correlations to all orders) relaxation to equilibrium from a *pinned* configuration. That is, we are interested in those initial configurations where either the first ($i = 1$) or the last ($i = N$) particle is pinned at x_0 , while the initial conditions of the remaining particles are drawn from the corresponding pinned equilibria (i.e. those equilibrium many-body configurations where the first/last particle is located at x_0).

We quantify the relaxation dynamics by means of $\mathcal{D}(t, x_{0i})$, the Kullback-Leibler divergence⁸⁰ between the non-Markovian probability density of the tagged-particle's position at time t , $\mathcal{G}(x_i, t|x_{0i})$ in Eq. (7), and the respective equilibrium density $\mathcal{P}_{\text{eq}}(x_i) \equiv \lim_{t \rightarrow \infty} \mathcal{G}(x_i, t|x_{0i})$:

$$\mathcal{D}(t, x_{0i}) \equiv \int_{-\pi}^{\pi} dx \mathcal{G}(x, t|x_{0i}) \ln \left(\frac{\mathcal{G}(x, t|x_{0i})}{\mathcal{P}_{\text{eq}}(x)} \right). \quad (14)$$

In physical terms $\mathcal{D}(t, x_{0i})$ represents the displacement from equilibrium in the sense of an *excess instantaneous free energy*, i.e. $k_B T \mathcal{D}(t, x_{0i}) = F(t) - F^{81-83}$. Since the integral in Eq. (14) cannot be performed analytically we evaluate it numerically. We always pin the initial position of the tagged-particle at $x_0 = -2$. According to the effect of the pinning on

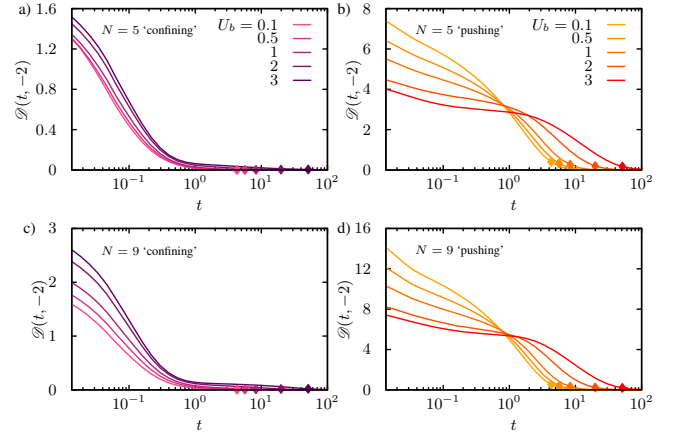


FIG. 4. Time evolution of $\mathcal{D}(t, x_{0i})$ for various barrier-heights U_b for $N = 5$ (a – confining; b – pushing) and $N = 9$ (c – confining; d – pushing), respectively. The symbols denote $\mathcal{D}(\Lambda_1^{-1}, x_{0i})$.

the relaxation of the tagged-particle, the scenario in which we tag the first particle is referred to as '*confining*' (since background particles obstruct the relaxation of the tagged-particle) and the one in which we tag the first particle as '*pushing*' (since background particles exert an entropic force pushing the tagged-particle over the barrier). $\mathcal{D}(t, x_{0i})$ as a function of the barrier height U_b for $N = 5$ and $N = 9$ is shown in Fig. 4.

Note that $\lim_{t \rightarrow 0} \mathcal{D}(t, x_{0i}) = \infty$ irrespective of N and U_b since we are comparing a delta distribution with a smooth probability density. Conversely, in an arbitrarily small time interval $\tau_\epsilon > 0$ the non-Markovian tagged-particle density $\mathcal{G}(x, t|x_{0i})$ evolves to a smooth, well-behaved probability density such that $\mathcal{D}(t > 0, x_{0i})$ is always finite and the 'pathology' at $t = 0$ is mathematical and not physical.

With this in mind we observe in Fig. 4 a striking difference between the 'confining' and 'pushing' scenario. In the 'confining' setting $\mathcal{D}(t, x_{01})$ at a fixed time t is a monotonically increasing function of U_b and as a function of time decays on a time-scale that seems to be rather independent of U_b . In the 'confining' scenario an increase of U_b displaces the system at $t = 0^+$ further from equilibrium. This is intuitive because $\mathcal{P}_{\text{eq}}(x_1)$ becomes more strongly confined to the boundary and hence away from x_0 . To a dominant extent relaxation occurs already on time-scales $t \gtrsim 1 \ll \Lambda_1^{-1}$. The reason may be found in the fact that Λ_1^{-1} corresponds to the mixing/ergodic time-scale on which the full single-file (and thus the tagged-particle) explores the entire system. In the 'confining' scenario the background particles are drawn from a distribution that resembles closely the unconstrained equilibrium and, in addition, the tagged-particle is nominally unlikely to be found in the right well in equilibrium. Therefore, the fraction of paths that cross the barrier in the ensemble of relaxation paths is small, rendering $V_{0\mathbf{k}}V_{\mathbf{k}0}$ for low-lying \mathbf{k} essentially negligible (see Eq. (7)). Nevertheless, a second, slower relaxation stage is still discernible at $t \gtrsim 1$.

Conversely, in the 'pushing' scenario depicted in Fig. 4b and 4d we find (i) the dependence of $\mathcal{D}(0^+, x_{01})$ on U_b to be inverted, and (ii) for given N and U_b relaxation extends

to much longer time-scales compared to the 'confining' scenario. In order to rationalize (i) we consider a pair of barriers U_{b_1}, U_{b_2} and take the limit

$$\lim_{t \rightarrow 0} (\mathcal{D}^{b_1}(t, x_0) - \mathcal{D}^{b_2}(t, x_0)) = \ln \left(\mathcal{P}_{\text{eq}}^{b_2}(x_0) / \mathcal{P}_{\text{eq}}^{b_1}(x_0) \right), \quad (15)$$

which is finite and well defined despite the fact that $\lim_{t \rightarrow 0} \mathcal{D}^{b_1, b_2}(t, x_0)$ are infinite. Eq. (15) explains that the dependence of $\mathcal{D}(0^+, x_0)$ on U_b is not unique and depends on the pinning point x_0 which determines whether or not $\mathcal{P}_{\text{eq}}^{b_2}(x_0) / \mathcal{P}_{\text{eq}}^{b_1}(x_0)$ is greater or smaller than 1 (see Fig. 1b and 1d). (ii) can be understood by an extension of the argument put forward in the discussion of the 'confining' scenario, i.e. as a result of the pinning the initial configurations of the background particles are displaced much further away from equilibrium, rendering $V_{0\mathbf{k}} V_{\mathbf{k}0}$ for low-lying \mathbf{k} substantial (see Eq. (7)). Therefore, a pronounced second relaxation stage is visible at longer times $t \gtrsim 1$.

Based on Fig. 4 alone we are not able to deduce whether these observations are a trivial consequence of the pinning in the sense that they have nothing to do with memory (note that a Markov process 'remembers' the initial condition up to $\sim \tau_{\text{rel}}$) or whether they are in fact a signature of memory in the dynamics. Additional insight is gained by inspecting the relaxation of the full, Markovian single-file evolving from the same initial condition, i.e.

$$\mathcal{D}_M(t, x_0) \equiv \left[\prod_{i=1}^N \int_{-\pi}^{\pi} dx_i \right] G(\mathbf{x}, t, P_0) \ln \left(\frac{G(\mathbf{x}, t, P_0)}{P_{\text{eq}}(\mathbf{x})} \right), \quad (16)$$

where we have introduced the joint Markovian two-point probability density $G(\mathbf{x}, t, P_0) \equiv \int d\mathbf{y}_0 G(\mathbf{x}, t | \mathbf{y}_0) P_0(\mathbf{y}_0)$ whereby, for $-\pi < x_0 < -\pi/2$, $P_0(\mathbf{y})$ is defined as

$$P_0(\mathbf{x}) = N! (\pi + x_0)^{-N_L} \hat{O}_{\mathbf{x}} \delta(x_i - x_0) \frac{e^{-U_b \sum_{j=i+1}^N \theta(\pi/2 - |x_j|)}}{(\pi e^{-U_b} - x_0)^{N_R}}, \quad (17)$$

where $\theta(x)$ is the Heaviside step function, and $P_{\text{eq}}(\mathbf{x}) = \lim_{t \rightarrow \infty} G(\mathbf{x}, t | \mathbf{x}_0)$. The integration in Eq. (16) can be performed analytically (for details please see Ref. 83). Introducing the two-point joint density of the single-particle problem $\Gamma_t(x, a, b) \equiv \sum_k \psi_k^R(x) [\int_a^b dy \psi_k^L(y) P_0(y)] e^{-\lambda_k t}$ with $P_0(y) \equiv \theta(-\pi/2 - y) / (\pi + x_0) + \theta(y + \pi/2) e^{-U(y)} / (\pi e^{-U_b} - x_0)$ as well as the auxiliary function

$$\Xi_t(a, b) = \int_a^b dx \Gamma_t(x, a, b) \ln(\Gamma_t(x, a, b) / P_{\text{eq}}(x)), \quad (18)$$

where $P_{\text{eq}}(x) = e^{-U(x)} / \pi(1 + e^{-U_b})$, the result reads

$$\mathcal{D}_M(t, x_0) = \Xi_t(-\pi, \pi) \Xi_t(-\pi, x_0)^{N_L} \Xi_t(x_0, \pi)^{N_R}. \quad (19)$$

An explicit solution is obtained with the aid of Mathematica⁸⁴. As it is bulky but straightforward we do not show it here. The Markovian result in Eq. (19) for the same set of parameters as in Fig. 4a and 4b is depicted in Fig. 5. A comparison of Figs. 4 and 5 reveals that the second, long-time relaxation stage observed in the 'pushing' scenario in Fig. 4 is absent in the Markovian setting (compare Figs. 4 and 5 and note

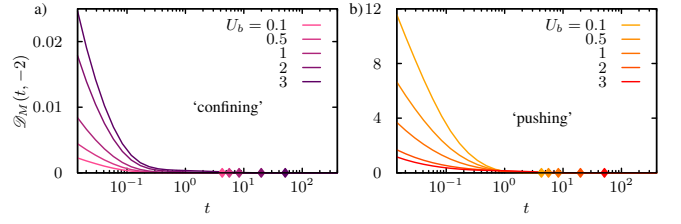


FIG. 5. Time evolution of $\mathcal{D}_M(t, x_{0i})$ for various barrier-heights U_b for $N = 5$ (a – confining, $i = 1$; b – pushing, $i = N$). The symbols denote $\mathcal{D}_M(\Lambda_1^{-1}, x_{0i})$.

that the relaxation time Λ_1^{-1} is identical in both settings). This in turn implies that the pronounced second relaxation stage in the non-Markovian, tagged-particle scenario at times $t \gtrsim 1$ is indeed a signature of memory.

V. DISCUSSION

We identified pronounced signatures of memory in the overdamped relaxation of a tagged-particle in a single-file confined to a bi-stable potential. On the level of linear correlations in equilibrium memory is visible in the form of a multi-scale relaxation of the autocorrelation function (see Fig. 2) and a seemingly paradoxical shortening of the so-called correlation time T_c (see Fig. 3). The latter was shown to be an artifact of the definition of T_c . When including the complete correlation-structure as encoded in the so-called excess instantaneous free energy (see Eq. (14)) distinctive signatures of memory emerge in the form of a second, late-time relaxation regime.

The memory originates from the fact that the entire single-file relaxes to equilibrium in the form of linearly independent many-body eigenmodes, which become projected on the motion of a tagged particle^{35,71}. The projection couples distinct modes thus breaking Markovianity and giving rise to memory³⁵. It turns out to be very important which particle is tagged. Here, we were only interested in the 'confining' (all background particles in front of the tagged particle) and 'pushing' (all background particles behind the tagged particle) scenarios and found qualitatively different relaxation behavior. A systematic analysis would be required to understand the intricate details in how the number of particles on each side affects relaxation dynamics, which is beyond the scope of this Communication.

Our results can readily be tested by existing experiments probing colloidal particle systems (see e.g.^{85–87}), and may furthermore be relevant for a theoretical description of transport in ion-channels^{88–91}. Our results can be extended in diverse ways, most immediately by including other types of inter-particle interactions⁹² and time-dependent energy barriers⁹³.

VI. APPENDIX

In this Appendix we give explicit expressions for the single-particle eigenfunctions that are required in the diagonalization of the many-body Fokker-Planck operator using the so-called coordinate Bethe ansatz. For details of the solution method please see^{35,71,75}). The eigenfunctions of the corresponding single-particle eigenvalue problem

$$\begin{aligned} (\partial_x^2 + \partial_x \{ \partial_x U(x) \}) \psi_k^R(x) &= -\lambda_k \psi_k^R(x) \\ (\partial_x^2 - \{ \partial_x U(x) \} \partial_x) \psi_k^L(x) &= -\lambda_k \psi_k^L(x), \end{aligned} \quad (20)$$

where $\psi_k^{L,R}(x) : [-\pi, \pi] \rightarrow \mathbb{R}$ allow for a spectral decomposition of the single-particle Green's function

$$\Gamma(x, t | x_0) = \sum_k \psi_k^R(x) \psi_k^L(x_0) e^{-\lambda_k t}. \quad (21)$$

$\psi_k^{L,R}(x)$ enter Eq. (5) and are here defined via their 'Hermitianized' counterpart $\psi_k(x) : [-\pi, \pi] \rightarrow \mathbb{R}$ as $\psi_k^R(x) = e^{-U(x)/2} \psi_k(x)$, $\psi_k^L(x) = e^{U(x)/2} \psi_k(x)$ where⁹⁴

$$\psi_k(x) = \sqrt{\frac{2}{1 + \delta_{k,0}}} \frac{e^{-U(x)/2}}{\sqrt{\pi(1 + e^{-f_0})}} \cos(\sqrt{\lambda_k} x), \quad \text{mod}(k, 4) = 0 \quad (22)$$

$$\psi_k(x) = \begin{cases} -\frac{\cos(\sqrt{\lambda_k}(x + \pi))}{\sqrt{\pi}}, & x < -\pi/2 \\ \frac{\sin(\sqrt{\lambda_k} x)}{\sqrt{\pi}}, & |x| \leq \pi/2 \\ \frac{\cos(\sqrt{\lambda_k}(x - \pi))}{\sqrt{\pi}}, & x > \pi/2 \end{cases}, \quad \text{mod}(k, 4) = 1 \quad (23)$$

$$\psi_k(x) = \sqrt{2} \frac{e^{U(x)/2}}{\sqrt{\pi(1 + e^{f_0})}} \cos(\sqrt{\lambda_k} x), \quad \text{mod}(k, 4) = 2 \quad (24)$$

$$\psi_k(x) = \begin{cases} \frac{\cos(\sqrt{\lambda_k}(x + \pi))}{\sqrt{\pi}}, & x < -\pi/2 \\ \frac{\sin(\sqrt{\lambda_k} x)}{\sqrt{\pi}}, & |x| \leq \pi/2 \\ -\frac{\cos(\sqrt{\lambda_k}(x - \pi))}{\sqrt{\pi}}, & x > \pi/2 \end{cases}, \quad \text{mod}(k, 4) = 3, \quad (25)$$

where $\delta_{k,0}$ is the Kronecker delta.

ACKNOWLEDGMENTS

The financial support from the German Research Foundation (DFG) through the Emmy Noether Program GO 2762/1-1 (to AG) is gratefully acknowledged. We thank Kristian Blom for fruitful discussions.

DATA AVAILABILITY

The data that support the findings of this study are available from the corresponding author upon reasonable request. An extension of the code published in Ref. 75 that implements the analytical results presented in this manuscript is included in the Supplementary Material.

REFERENCES

- ¹H.A. Kramers. Brownian motion in a field of force and the diffusion model of chemical reactions. *Physica*, 7(4):284–304, April 1940.
- ²Abraham Nitzan, Peter Ortoleva, John Deutch, and John Ross. Fluctuations and transitions at chemical instabilities: The analogy to phase transitions. *J. Chem. Phys.*, 61(3):1056–1074, 1974.
- ³F. Schlögl. Chemical reaction models for non-equilibrium phase transitions. *Z. Physik*, 253(2):147–161, Apr 1972.
- ⁴I. Matheson, D. F. Walls, and C. W. Gardiner. Stochastic models of firstorder nonequilibrium phase transitions in chemical reactions. *J. Stat. Phys.*, 12(1):21–34, Jan 1975.
- ⁵Rolf Landauer. The role noise in negative resistance circuits. *J. Phys. Soc. Jpn.*, 41(2):695–696, 1976.
- ⁶H. Risken. Distribution- and correlation-functions for a laser amplitude. *Z. Physik*, 186(1):85–98, Feb 1965.
- ⁷Ryogo Kubo, Kazuhiro Matsuo, and Kazuo Kitahara. Fluctuation and relaxation of macrovariables. *J. Stat. Phys.*, 9(1):51–96, Sep 1973.
- ⁸H. Lannon, J. S. Haghpahanah, J. K. Montclare, E. Vanden-Eijnden, and J. Brujic. Force-Clamp Experiments Reveal the Free-Energy Profile and Diffusion Coefficient of the Collapse of Protein Molecules. *Phys. Rev. Lett.*, 110(12):128301, March 2013.
- ⁹Hoi Sung Chung and William A Eaton. Protein folding transition path times from single molecule FRET. *Curr. Opin. Struct. Biol.*, 48:30–39, February 2018.
- ¹⁰H. Yu, A. N. Gupta, X. Liu, K. Neupane, A. M. Brigley, I. Sosova, and M. T. Woodside. Energy landscape analysis of native folding of the prion protein yields the diffusion constant, transition path time, and rates. *Proc. Natl. Acad. Sci. USA*, 109(36):14452–14457, September 2012.
- ¹¹Ajay P. Manuel, John Lambert, and Michael T. Woodside. Reconstructing folding energy landscapes from splitting probability analysis of single-molecule trajectories. *Proc. Natl. Acad. Sci. USA*, 112(23):7183–7188, June 2015.
- ¹²Katherine Truex, Hoi Sung Chung, John M. Louis, and William A. Eaton. Testing Landscape Theory for Biomolecular Processes with Single Molecule Fluorescence Spectroscopy. *Phys. Rev. Lett.*, 115(1):018101, July 2015.
- ¹³H. S. Chung, K. McHale, J. M. Louis, and W. A. Eaton. Single-Molecule Fluorescence Experiments Determine Protein Folding Transition Path Times. *Science*, 335(6071):981–984, February 2012.
- ¹⁴David de Sancho, Anshul Sirur, and Robert B. Best. Molecular origins of internal friction effects on protein-folding rates. *Nat. Commun.*, 5(1):4307, September 2014.
- ¹⁵Robert Best and Gerhard Hummer. Diffusive Model of Protein Folding Dynamics with Kramers Turnover in Rate. *Phys. Rev. Lett.*, 96(22):228104, June 2006.
- ¹⁶Julian Kappler, Jan O. Daldrop, Florian N. Brünig, Moritz D. Boehle, and Roland R. Netz. Memory-induced acceleration and slowdown of barrier crossing. *J. Chem. Phys.*, 148(1):014903, 2018.
- ¹⁷Krishna Neupane, Ajay P. Manuel, John Lambert, and Michael T. Woodside. Transition-Path Probability as a Test of Reaction-Coordinate Quality Reveals DNA Hairpin Folding Is a One-Dimensional Diffusive Process. *J. Phys. Chem. Lett.*, 6(6):1005–1010, March 2015.
- ¹⁸K. Neupane, D. A. N. Foster, D. R. Dee, H. Yu, F. Wang, and M. T. Woodside. Direct observation of transition paths during the folding of proteins and nucleic acids. *Science*, 352(6282):239–242, April 2016.
- ¹⁹Felix Rico, Andreas Russek, Laura González, Helmut Grubmüller, and Simon Scheuring. Heterogeneous and rate-dependent streptavidin–biotin un-

- binding revealed by high-speed force spectroscopy and atomistic simulations. *Proc. Natl. Acad. Sci. USA*, 116(14):6594–6601, April 2019.
- ²⁰N. G. van Kampen. A soluble model for diffusion in a bistable potential. *J. Stat. Phys.*, 17(2):71–88, Aug 1977.
- ²¹B. Caroli, C. Caroli, and B. Roulet. Diffusion in a bistable potential: A systematic wkb treatment. *J. Stat. Phys.*, 21(4):415–437, Oct 1979.
- ²²Yukio Saito. Relaxation in a bistable system. *J. Phys. Soc. Jpn.*, 41(2):388–393, Aug 1976.
- ²³Armin Bunde and Jean-François Gouyet. Brownian motion in the bistable potential at intermediate and high friction: Relaxation from the instability point. *Physica A*, 132(2):357–374, 1985.
- ²⁴Peter Hanggi, Hermann Grabert, Peter Talkner, and Harry Thomas. Bistable systems: Master equation versus fokker-planck modeling. *Phys. Rev. A*, 29:371–378, Jan 1984.
- ²⁵Angelo Perico, Roberto Prato-longo, Karl F. Freed, Richard W. Pastor, and Attila Szabo. Positional time correlation function for one-dimensional systems with barrier crossing: Memory function corrections to the optimized Rouse–Zimm approximation. *J. Chem. Phys.*, 98(1):564–573, January 1993.
- ²⁶Angelo Perico, Roberto Prato-longo, Karl F. Freed, and Attila Szabo. Torsional time correlation function for one-dimensional systems with barrier crossing: Periodic potential. *J. Chem. Phys.*, 101(3):2554–2561, August 1994.
- ²⁷Peter Hänggi, Peter Talkner, and Michal Borkovec. Reaction-rate theory: fifty years after Kramers. *Rev. Mod. Phys.*, 62(2):251–341, April 1990.
- ²⁸B.U. Felderhof. Escape by diffusion from a square well across a square barrier. *Physica A*, 387(1):39–56, January 2008.
- ²⁹V. Berdichevsky and M. Gitterman. One-dimensional diffusion through single- and double-square barriers. *J. Phys. A: Math. Gen.*, 29(8):1567–1580, April 1996.
- ³⁰Bokkyoo Jun and David L. Weaver. One-dimensional potential barrier model of protein folding with intermediates. *J. Chem. Phys.*, 116(1):418, 2002.
- ³¹Graham R. Fleming, Scott H. Courtney, and Michael W. Balk. Activated barrier crossing: Comparison of experiment and theory. *J. Stat. Phys.*, 42(1-2):83–104, January 1986.
- ³²Alexander M. Berezhkovskii and Dmitrii E. Makarov. Communication: Transition-path velocity as an experimental measure of barrier crossing dynamics. *J. Chem. Phys.*, 148(20):201102, May 2018.
- ³³David Hartich and Aljaž Godec. Duality between relaxation and first passage in reversible Markov dynamics: rugged energy landscapes disentangled. *New J. Phys.*, 20(11):112002, November 2018.
- ³⁴David Hartich and Aljaž Godec. Interlacing relaxation and first-passage phenomena in reversible discrete and continuous space markovian dynamics. *J. Stat. Mech.*, 2019(2):024002, Feb 2019.
- ³⁵Alessio Lapolla and Aljaž Godec. Manifestations of Projection-Induced Memory: General Theory and the Tilted Single File. *Front. Phys.*, 7, 2019.
- ³⁶N.G. van Kampen. Remarks on Non-Markov Processes. *Braz. J. Phys.*, 28(2), June 1998.
- ³⁷Peter Hanggi and Fatemeh Mojtabai. Thermally activated escape rate in presence of long-time memory. *Phys. Rev. A*, 26(2):1168–1170, August 1982.
- ³⁸Shoichi Okuyama and David W. Oxtoby. The generalized Smoluchowski equation and non-Markovian dynamics. *J. Chem. Phys.*, 84(10):5824–5829, May 1986.
- ³⁹Shoichi Okuyama and David W. Oxtoby. Non-Markovian dynamics and barrier crossing rates at high viscosity. *J. Chem. Phys.*, 84(10):5830–5835, May 1986.
- ⁴⁰Benny Carmeli and Abraham Nitzan. Non-Markoffian Theory of Activated Rate Processes. *Phys. Rev. Lett.*, 49(7):423–426, August 1982.
- ⁴¹Benny Carmeli and Abraham Nitzan. Non-Markovian theory of activated rate processes. I. Formalism. *J. Chem. Phys.*, 79(1):393–404, July 1983.
- ⁴²Benny Carmeli and Abraham Nitzan. Non-Markovian theory of activated rate processes. IV. The double well model. *J. Chem. Phys.*, 80(8):3596–3605, April 1984.
- ⁴³V. I. Mel’nikov and S. V. Meshkov. Theory of activated rate processes: Exact solution of the Kramers problem. *J. Chem. Phys.*, 85(2):1018–1027, July 1986.
- ⁴⁴Yu. P. Kalmykov, W. T. Coffey, and S. V. Titov. Thermally activated escape rate for a Brownian particle in a double-well potential for all values of the dissipation. *J. Chem. Phys.*, 124(2):024107, January 2006.
- ⁴⁵Richard F. Grote and James T. Hynes. The stable states picture of chemical reactions. II. Rate constants for condensed and gas phase reaction models. *J. Chem. Phys.*, 73(6):2715–2732, September 1980.
- ⁴⁶David Chandler. Statistical mechanics of isomerization dynamics in liquids and the transition state approximation. *J. Chem. Phys.*, 68(6):2959, 1978.
- ⁴⁷Julian Kappeler, Victor B. Hinrichsen, and Roland R. Netz. Non-Markovian barrier crossing with two-time-scale memory is dominated by the faster memory component. *Eur. Phys. J. E*, 42(9):119, September 2019.
- ⁴⁸Sean L. Seyler and Steve Pressé. Surmounting potential barriers: Hydrodynamic memory hedges against thermal fluctuations in particle transport. *J. Chem. Phys.*, 153(4):041102, Jul 2020.
- ⁴⁹Andrew G. T. Pyo and Michael T. Woodside. Memory effects in single-molecule force spectroscopy measurements of biomolecular folding. *Phys. Chem. Chem. Phys.*, 21(44):24527–24534, 2019.
- ⁵⁰P. Hänggi, F. Marchesoni, and P. Grigolini. Bistable flow driven by coloured gaussian noise: A critical study. *Z. Physik B - Condensed Matter*, 56(4):333–339, Dec 1984.
- ⁵¹Peter Hänggi. Path integral solutions for non-markovian processes. *Z. Physik B - Condensed Matter*, 75(2):275–281, Jun 1989.
- ⁵²Ronald F. Fox. Functional-calculus approach to stochastic differential equations. *Phys. Rev. A*, 33:467–476, Jan 1986.
- ⁵³Charles R. Doering, Patrick S. Hagan, and C. David Levermore. Bistability driven by weakly colored gaussian noise: The fokker-planck boundary layer and mean first-passage times. *Phys. Rev. Lett.*, 59:2129–2132, Nov 1987.
- ⁵⁴J. Casademunt, R. Mannella, P. V. E. McClintock, F. E. Moss, and J. M. Sancho. Relaxation times of non-markovian processes. *Phys. Rev. A*, 35:5183–5190, Jun 1987.
- ⁵⁵G. Hummer, J. C. Rasaiah, and J. P. Noworyta. Water conduction through the hydrophobic channel of a carbon nanotube. *Nature*, 414(6860):188–190, November 2001.
- ⁵⁶Tom Chou and Detlef Lohse. Entropy-Driven Pumping in Zeolites and Biological Channels. *Phys. Rev. Lett.*, 82(17):3552–3555, April 1999.
- ⁵⁷Sebastian Ahlberg, Tobias Ambjörnsson, and Ludvig Lizana. Many-body effects on tracer particle diffusion with applications for single-protein dynamics on DNA. *New J. Phys.*, 17(4):043036, apr 2015.
- ⁵⁸Gene-Wei Li, Otto G. Berg, and Johan Elf. Effects of macromolecular crowding and DNA looping on gene regulation kinetics. *Nat. Phys.*, 5(4):294–297, April 2009.
- ⁵⁹Peter M. Richards. Theory of one-dimensional hopping conductivity and diffusion. *Phys. Rev. B*, 16(4):1393–1409, August 1977.
- ⁶⁰Alessandro Taloni, Ophir Flomenbom, Ramón Castañeda-Priego, and Fabio Marchesoni. Single file dynamics in soft materials. *Soft Matter*, 13(6):1096–1106, 2017.
- ⁶¹T. E. Harris. Diffusion with “collisions” between particles. *J. Appl. Probab.*, 2(2):323–338, December 1965.
- ⁶²D. W. Jepsen. Dynamics of a Simple Many-Body System of Hard Rods. *J. Math. Phys.*, 6(3):405–413, March 1965.
- ⁶³L. Lizana and T. Ambjörnsson. Single-File Diffusion in a Box. *Phys. Rev. Lett.*, 100(20):200601, May 2008.
- ⁶⁴L. Lizana and T. Ambjörnsson. Diffusion of finite-sized hard-core interacting particles in a one-dimensional box: Tagged particle dynamics. *Phys. Rev. E*, 80(5):051103, November 2009.
- ⁶⁵E. Barkai and R. Silbey. Theory of Single File Diffusion in a Force Field. *Phys. Rev. Lett.*, 102(5):050602, February 2009.
- ⁶⁶E. Barkai and R. Silbey. Diffusion of tagged particle in an exclusion process. *Phys. Rev. E*, 81(4):041129, April 2010.
- ⁶⁷N. Leibovich and E. Barkai. Everlasting effect of initial conditions on single-file diffusion. *Phys. Rev. E*, 88(3):032107, September 2013.
- ⁶⁸O. Flomenbom and A. Taloni. On single-file and less dense processes. *Europhys. Lett.*, 83(2):20004, July 2008.
- ⁶⁹R. Metzler, L. Sanders, M. A. Lomholt, L. Lizana, K. Fogelmark, and Tobias Ambjörnsson. Ageing single file motion. *Eur. Phys. J. Spec. Top.*, 223(14):3287–3293, December 2014.
- ⁷⁰Ludvig Lizana, Tobias Ambjörnsson, Alessandro Taloni, Eli Barkai, and Michael A. Lomholt. Foundation of fractional Langevin equation: Harmonization of a many-body problem. *Phys. Rev. E*, 81(5):051118, May 2010.
- ⁷¹Alessio Lapolla and Aljaž Godec. Unfolding tagged particle histories in single-file diffusion: exact single- and two-tag local times beyond large

- deviation theory. *New J. Phys.*, 20(11):113021, November 2018.
- ⁷²S. D. Goldt and E. M. Terentjev. Role of the potential landscape on the single-file diffusion through channels. *J. Chem. Phys.*, 141(22):224901, Dec 2014.
- ⁷³M. Morsch, H. Risken, and H. D. Vollmer. One-dimensional diffusion in soluble model potentials. *Z Physik B*, 32(2):245–252, June 1979.
- ⁷⁴Hannes Risken and Till Frank. *The Fokker-Planck Equation: Methods of Solution and Applications*. Springer Series in Synergetics. Springer-Verlag, Berlin Heidelberg, 2 edition, 1996.
- ⁷⁵Alessio Lapolla and Aljaz Godec. BetheSF: Efficient computation of the exact tagged particle propagator in single file systems via the Bethe eigenspectrum. *Comput. Phys. Commun.*, March 2020. (accepted for publication).
- ⁷⁶https://www.boost.org/doc/libs/1_71_0/libs/math/doc/html/quadrature.html (20/09/2019).
- ⁷⁷Note that Eqs. (5-9) imply that a_k is a positive constant times the square of a real number.
- ⁷⁸Giovanni Lipari and Attila Szabo. Model-free approach to the interpretation of nuclear magnetic resonance relaxation in macromolecules. 1. Theory and range of validity. *J. Am. Chem. Soc.*, 104(17):4546–4559, August 1982.
- ⁷⁹Note that τ_{rel} does not depend on N .
- ⁸⁰S. Kullback and R. Leibler. On information and sufficiency. *Ann. Math. Statist.*, 22(1):79–86, 1951.
- ⁸¹Michael C. Mackey. The dynamic origin of increasing entropy. *Rev. Mod. Phys.*, 61(4):981–1015, Oct 1989.
- ⁸²Hong Qian. A decomposition of irreversible diffusion processes without detailed balance. *J. Math. Phys.*, 54(5):053302, May 2013.
- ⁸³Alessio Lapolla and Aljaz Godec. Faster uphill relaxation in thermodynamically equidistant temperature quenches. *Phys. Rev. Lett.*, accepted (arXiv:2002.08237), 2020.
- ⁸⁴Wolfram Research, Inc. Mathematica, Version 12.0, 2019.
- ⁸⁵Q.-H. Wei, C. Bechinger, and P. Leiderer. Single-file diffusion of colloids in one-dimensional channels. *Science*, 287(5453):625–627, 2000.
- ⁸⁶Richard D. L. Hanes, Cécile Dalle-Ferrier, Michael Schmiedeberg, Matthew C. Jenkins, and Stefan U. Egelhaaf. Colloids in one dimensional random energy landscapes. *Soft Matter*, 8(9):2714, 2012.
- ⁸⁷Alice L. Thorneywork, Jannes Gladrow, Yujia Qing, Marc Rico-Pasto, Felix Ritort, Hagan Bayley, Anatoly B. Kolomeisky, and Ulrich F. Keyser. Direct detection of molecular intermediates from first-passage times. *Sci. Adv.*, 6(18):eaaz4642, May 2020.
- ⁸⁸Benoît Roux, Toby Allen, Simon Bernèche, and Wonpil Im. Theoretical and computational models of biological ion channels. *Quart. Rev. Biophys.*, 37(1):15–103, February 2004.
- ⁸⁹Andrew Pohorille, Michael A. Wilson, and Chenyu Wei. Validity of the Electrodiffusion Model for Calculating Conductance of Simple Ion Channels. *J. Phys. Chem. B*, 121(15):3607–3619, April 2017.
- ⁹⁰Wojciech Kopec, David A. Köpfer, Owen N. Vickery, Anna S. Bondarenko, Thomas L. C. Jansen, Bert L. de Groot, and Ulrich Zachariae. Direct knock-on of desolvated ions governs strict ion selectivity in K⁺ channels. *Nature Chem.*, 10(8):813–820, August 2018.
- ⁹¹Razi Epsztein, Ryan M. DuChanois, Cody L. Ritt, Aleksandr Noy, and Menachem Elimelech. Towards single-species selectivity of membranes with subnanometre pores. *Nat. Nanotechnol.*, 15(6):426–436, June 2020.
- ⁹²Markus Kollmann. Single-file diffusion of atomic and colloidal systems: Asymptotic laws. *Phys. Rev. Lett.*, 90:180602, May 2003.
- ⁹³Evzen Subrt and Petr Chvosta. Diffusion in the time-dependent double-well potential. *Czech J Phys*, 56(2):125–139, February 2006.
- ⁹⁴We here correct typos found in the original publications.